Nanoscale



COMMUNICATION

View Article Online
View Journal | View Issue



Cite this: Nanoscale, 2019, 11, 2617

Received 25th August 2018, Accepted 16th January 2019 DOI: 10.1039/c8nr06890a

rsc.li/nanoscale



Zhikun Liu, (Da,b Siyu Liu,a Wenzhuo Wu (D*a,c and C. Richard Liu*a,c

Laser-induced chemical deposition is an economical "grow-inplace" approach to produce functional materials. The lack of precise control over the component density and other properties hinders the development of the method towards an efficient nanomanufacturing technology. In this paper, we provide a mechanism of direct pulsed-laser integration of ZnO nanowire seeding and growth on silicon wafers toward controlled density. Investigation of laser-induced ZnO nucleation directly deposited on a substrate suggested that the coverage percentage of nucleus particles was a function of instantly available area, supplementing the classical nucleation theory for confined area deposition. A processing window was found in which ZnO nanowires only grew from the early deposited nucleated particles as seeds. A study on ZnO nanowire growth showed that the process became transport limited over time, which was important for density-controlled nanowire growth integrated on nucleated seeds. The proposed mechanism provided guidance to integrate nanomaterials using laser-induced chemical deposition with a controlled density and morphology.

Introduction

Laser-induced chemical deposition^{1–8} could synthesize and directly integrate ("grow-in-place"⁹) numerous functional nanomaterials without the need to perform a series of procedures in conventional nanomaterial growth processes (*e.g.*, photolithography, seed deposition, lift-off, growth, *etc.*). Moreover, each process in those conventional methods is time consuming. In contrast, the laser technique provides a facile approach to grow and integrate nanomaterials economically with micron-scale precision. The growth rate of nanotubes¹ or nanowires^{2–6} by the laser process was significantly higher than

those by conventional methods. With rapid developments of the parallel laser processing technology, 10-14 laser-induced chemical deposition is a promising method for scale-up production and integration of nanomaterials.

For practical applications, the density and other topological, geometrical and functional properties of nanomaterials have strong impacts on the device performance. For example, the integration density of ZnO nanowires, a multi-functional nanomaterial of numerous application interest, can significantly affect the performance of related devices. Therefore, the related fundamental understanding and technological capability in manufacturing is crucial and pressing 1,120 for advancing the laser processes.

Compared to the continuous-wave laser widely used for growing ZnO nanowires, ⁵⁻⁸ the use of a pulsed laser ¹⁻⁴ could advance both the fundamental understanding and technological capability in integrating seeding and growing nanowires. This is because a pulsed laser has many more parameters available for control and tuning. Among others, many controlled variations of temperature can be generated in a duration of nano-, pico-, and femto-seconds by a pulsed laser to help study and identify the values of multiple energy barriers in nucleation/growth which are important in nanomanufacturing science for improving the productivity and quality of related materials.

Nevertheless, a pathway for the pulsed-laser-induced chemical deposition and integration of nanomaterials (e.g., ZnO nanowires) and a fundamental understanding of the related mechanism are lacking. Our work addressed these fundamental aspects and identified for the first time the mechanism for pulsed-laser-induced nucleation and growth of ZnO nanowires. In this paper, we report the controlled integration of ZnO nanowires by pulsed-laser-induced chemical deposition and discuss its mechanism. The growth of nanowires was obtained on a more thermally conductive substrate (i.e., Si wafer) without the need for an additional seed layer. The control over the nanowire density was achieved by successfully decoupling the nucleation and crystal growth processes. Based on that, we were also able to provide insights into nucleation and nanowire growth individually.

^aSchool of Industrial Engineering, Purdue University, West Lafayette, Indiana 47907, USA. E-mail: wenzhuowu@purdue.edu, liuch@purdue.edu

^bSchool of Materials Science and Engineering, South China University of Technology, Guangzhou 510641. China

^cBirck Nanotechnology Center, Purdue University, West Lafayette, Indiana 47907, USA

Communication Nanoscale

Experimental

ZnO nanowires were deposited on a silicon (0001) substrate induced by a laser in a solution environment at room temperature. In this paper, the processes of ZnO nucleation and nanowire growth were studied separately. A high-frequency ytterbium-pulsed laser (1064 nm wavelength) was applied to initiate nucleation and induce nanowire growth. Laser energy was absorbed by the silicon substrate and thermally decomposed hexamethylenetetramine (HMTA) and provided the OHions for ZnO deposition.⁵ HMTA and zinc chloride (ZnCl₂) were dissolved in 50 ml deionized water, with diluted nitric acid (HNO₃, pH = 2.3) added to adjust the pH value of the solution. The solution for the nucleation process contained 6-22 mM ZnCl₂, 66 mM HMTA and 1 ml diluted nitric acid, and the solution for nanowire growth contained 22 mM ZnCl₂, 12 mM HMTA, and 6 ml-8 ml diluted nitric acid. In the nanoparticle formation step, a silicon substrate with a size of 1 cm × 1 cm was immersed in the solution. Then the substrate was irradiated with a pulsed laser (6 W, 50 kHz) with a beam size of 200 µm from the top through the aqueous solution, raising the temperature of the surrounding solution and initiating the reaction to form nanoparticles. If the heat were steadily generated and accumulated, the deposition of ZnO in the vicinity of the laser irradiation area would occur. To confine the deposition within the laser irradiation area, a moving plate was applied above the substrate to periodically block the laser irradiation and allow the generated heat to dissipate. Specifically, the substrate was exposed to the laser for 3 s (on time) to induce a chemical reaction and blocked for 20 s (off time) to prevent the heat accumulation. The total exposure time was 2 min for nanoparticle formation.

In the crystal growth step, the laser was operated under the same conditions but the blocking plate was not used. Compared to nucleation, the crystal growth process generally required a longer time to complete. Therefore, 1 hour steady laser (6 W) heating was applied for crystal growth. The nanowires grew upon the deposited nanoparticles in the first step. In order to eliminate the interference of additional nuclei on nanowire growth, an acid was added to inhibit nucleation in this step. Scanning electron microscopy (SEM, Hitachi 4800 Field-Emission) was used to observe ZnO nanoparticles and nanowire arrays. The nanoparticle/nanowire density was measured by SEM at 3 different positions. At each position, about 200 nanoparticles/nanowires were counted for the density estimation. The nanowire length was measured by cross-sectional or tilted-view SEM. In general, the length of nanowires appeared to be uniform. 30 nanowires were measured for each sample to calculate the average length.

Results and discussion

Controlled integration of ZnO nanowires

Fundamental studies on the growth of ZnO nanowires by the hydrothermal process have been conducted. 21-24 It was

believed that the chemical reactions for growing ZnO nanowires by a laser in solution were photothermal ones and similar to those by the hydrothermal process.^{5,6,8} The energy of the laser was absorbed by the silicon substrate which caused the temperature of the solution to rise. The decomposition of HMTA was accelerated locally by laser heating which produced ammonia. By hydrolysis of ammonia, hydroxide ions were produced. The reaction between Zn ions and hydroxide ions leads to the formation of ZnO. The chemical reactions can be presented as follows:²³

$$(CH_2)_6N_4 + 6H_2O \xrightarrow{heat} 6HCHO + 4NH_3$$
 (1)

$$NH_3 + H_2O \leftrightarrow NH_4^+ + OH^-$$
 (2)

$$2OH^- + Zn^{2+} \leftrightarrow ZnO + H_2O \tag{3}$$

The controlled integration was performed in two steps: nucleation/integration of ZnO nanoparticles and the growth of the nanoparticles to be nanowires, as shown in Fig. 1a. In general, compared to crystal growth, crystal nucleation, which is dominant at a high level of supersaturation, requires a shorter time to complete. Thus in the step of ZnO particle nucleation, laser irradiation chopped by a moving plate was employed to trigger the particle nucleation, while limiting the growth of the particle. Whereas in the step of nanowire growth, steady laser irradiation was used to produce constant thermal energy, supporting the nanowire growth. Selective growth of ZnO nanomaterials was achieved by spin-coated seeding and electron beam lithography, photolithography or microstamp methods which required multiple steps.²⁵ In this work, the deposition area of ZnO was confined directly by the laser beam. ZnO nanowires with different densities were integrated at the desired place of the silicon substrate without the need for a spin-coated seed layer, which prevented the contamination of ZnO in the unwanted regions. Fig. 1b1, b2 and b3, b4 show the SEM pictures of ZnO deposition after nanoparticle nucleation and after nanowire growth, respectively. The deposited spot areas of ZnO nanoparticles and nanowires were all around 200 µm in diameter, the same as the size of the laser beam. The densities of the integrated nanowire were determined by the density of the nanoparticles. When the density of nanoparticles was 4 × 108 cm⁻², free-standing nanowires of the same density were formed. The nanowires were 4 μm in height with a diameter of 800 nm, as shown in Fig. 1b4 and c4. The nanowires had a clear hexagonal structure, indicating a single crystalline wurtzite crystal structure. When the density reduced to 1×10^7 cm⁻², the distances between the particles increased, and many of the nanowires grew laterally along the substrate (see Fig. 1c1 and c2). If the density rose to 1 × 10¹⁰ cm⁻², a densely packed ZnO nanowire was obtained (see Fig. 1c6), forming a continuous thin film. The results were distinct from those in the early reports on the laser-induced deposition of ZnO in which only isolated nanowires were produced.^{5,6} By the laser process reported here, the diameter of integrated nanowires ranged from 200 nm to 800 nm and the length ranged from 200 nm to 4 µm, depend-

1 µm

(a) Laser (Chopped)

Blocking Plate

C3

C4

D3

Size: 200 µm

C5

C6

C6

C6

Nanoscale Communication

Fig. 1 Controlled integration of ZnO nanowires. (a) Schematic illustration of the experimental setup. (b) SEM pictures of ZnO deposition by laser-induced chemical deposition: (b1)(b2) integrated nanoparticles after laser-induced nucleation and (b3)(b4) integrated nanowires after laser-induced nanowire growth. (c) SEM pictures of controlled integration of nanowires: (c1)(c2) in low density, (c3)(c4) in medium density, and (c5)(c6) in high density.

ing on the processing conditions. The two-step laser-induced chemical deposition of the ZnO nanowire not only can integrate nanomaterials with a controlled density, but also provide unique opportunities to acquire a clearer understanding about nucleation and its influence on crystal growth.

Nanoparticle nucleation induced by a laser

During the step of nucleation/integration of ZnO nanoparticles, the substrate was under laser irradiation for 30 s and blocked from irradiation for 2 min. The laser heating effect caused the formation of hydroxide ions. The 2 min laser off time helped to prevent the accumulation of excess hydroxide ions and heat which leads to ZnO deposition in the vicinity of the laser beam. This is different from the conventional hydrothermal method in which the whole solution was continuously heated, making the kinetics of nucleation harder to control. Although laser irradiation with higher power can promote the ZnO nucleation, it can also result in too many hydroxide ions and delocalized the deposition. Therefore, the laser power was kept constant (6 W) in the studies of nanoparticle density control.

The dependence of particle density on precursor concentration and time was studied. We found that once the density of the particle was higher than 10⁸ cm⁻², agglomeration of nanoparticles occurred. The agglomeration phenomenon suggested that as the precursor concentration was raised for higher particle density, homogeneous nucleation above the substrate also took place during the particle formation

process. The agglomeration would interfere with the nanowire growth process. Here, we used a small amount (1 ml) of diluted acid (pH = 2.3) to inhibit the homogeneous nucleation while allowed the heterogeneous nucleation on a silicon substrate to occur. Therefore, nanoparticles with higher density could be formed without any particle agglomeration. By increasing the concentration of ZnCl₂ from 6 mM to 22 mM, the particle density can vary in a large range, from 1×10^7 cm^{-2} to 1×10^{10} cm⁻², as shown in Fig. 2a. At the same time, the particle size reduced from about 1 µm to 100 nm as the concentration of ZnCl2 increased from 6 mM to 22 mM. The nucleation phenomenon could be explained according to classical theory: as the supersaturation increased (higher concentration of ZnCl₂), the size of the critical nucleus was smaller, which resulted in smaller nanoparticles and the heterogeneous nucleation rate was higher, which lead to a higher density of nanoparticles.

The particle density gradually increased over time by laser-induced deposition. However, the increase rate gradually slowed down, which could not be explained by the classical nucleation model which only considers the temperature, pressure, and concentration of precursors. For deposition by a focused laser, the chemical reaction was confined in a micron-scale area, and inside the area, the coverage percentage (ZnO deposition area/confined reaction area) varied significantly over time. As shown in Fig. 2b, the average coverage percentages were 53%, 65%, 71% and 81% after 40 s, 1 min, 1 min 20 s and 2 min laser irradiation, respectively. Since the dur-

Communication

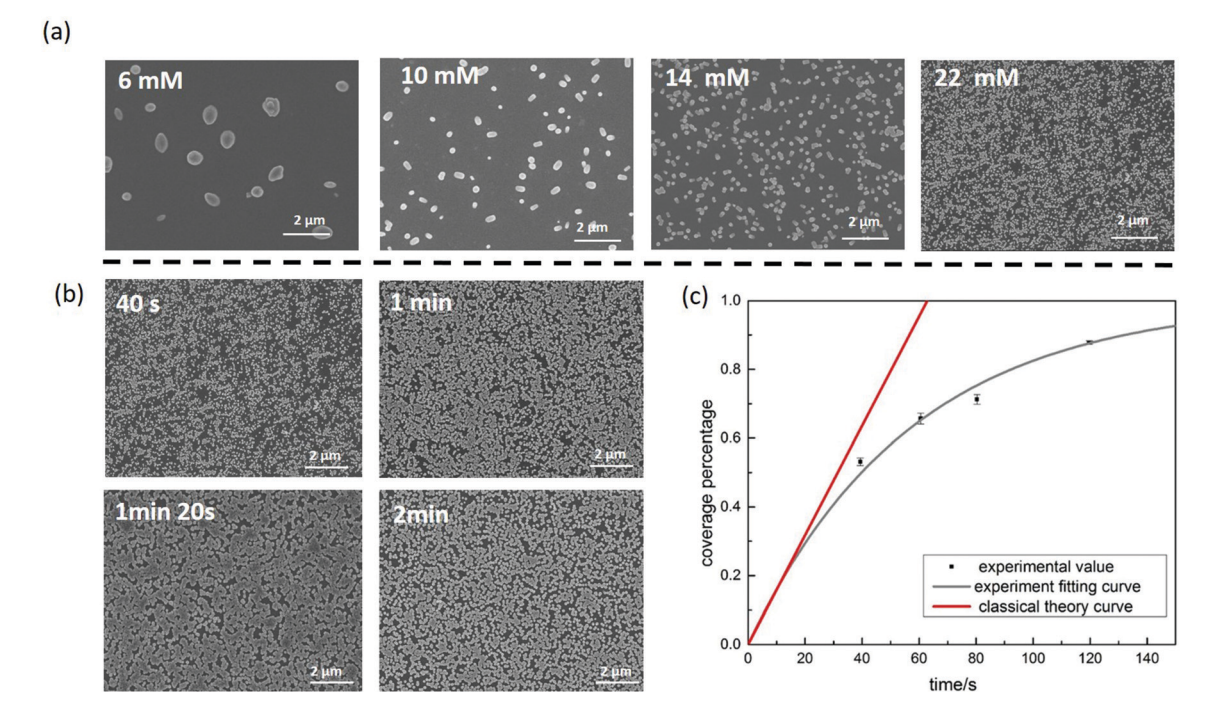


Fig. 2 Laser-induced ZnO nanoparticle nucleation/integration and density control. (a) SEM pictures of ZnO nanoparticles with different densities at different concentrations of ZnCl₂ 6 mM, 10 mM, 14 mM, and 22 mM, respectively. (b) SEM pictures of ZnO nanoparticles deposited at different deposition times 40 s, 1 min, 1 min and 20 s, and 2 min. (c) The relationship between nanoparticle coverage percentage and deposition time.

ation of laser irradiation was short (<2 min), the changes in the precursor concentration and temperature were believed to be minor. Therefore, the nucleation rate per available area was treated constantly. Here, a model was developed to describe the change of the area coverage percentage over time for laser-induced deposition in a confined area:

$$A \times (1 - x) \times R = A \times \frac{\mathrm{d}x}{\mathrm{d}t}$$

where A is the reaction area under laser irradiation, R is the 2D coverage area increase rate, defined as deposition area/(time × instant available area), and t represents time. $x = \frac{n \times S}{A}$ was defined as the area coverage percentage, where n is the number of nanoparticles and S is the area of nanoparticles. Therefore,

$$x = 1 - \exp(-R \times t)$$

By fitting the formula with the experiment data, the coverage percentage: $x = 1 - \exp(-0.017 \times t)$, as plotted in Fig. 2c. This model could explain the deceleration of the deposition rate that deviated from the prediction of the classical model. The deceleration was mainly attributed to the reduced instant available area over time. The model cannot describe the change of particle density over time unless the variation of particle size is known. In Fig. 2b, from 1 min to 1 min 20 s, the average size of the particle increased from 90 nm to 120 nm, whereas the average density decreased from $1.2 \times 10^{10} \ {\rm cm}^{-2}$ to $8 \times 10^9 \ {\rm cm}^{-2}$. It suggests that Ostwald ripening occurred simul-

taneously as the new deposition was made on the substrate, which was not considered in this model.

The process window for crystal growth without additional nucleation

A critical step towards the controlled integration of nanowires is the growth of the nanowire from the particle while preventing nucleation of the new particle (inside/outside the laser beam). Compared to the nucleation process, crystal growth required more time, therefore steady laser irradiation was preferred for nanowire growth. However, constant laser irradiation increases the possibility of nucleation of ZnO on new sites. Previously, a low conductivity of the substrate (such as a polymer) was used to confine the heating zone and hinder nucleation on the area outside the laser beam. The requirement on the substrate limits the applicability of the laser method.

Our strategy is to add a sufficient amount of acid to the solution to reduce the supersaturation of ZnO (reduce the concentration of OH⁻ in reaction (3) in order to shift the reaction to the left), therefore increasing the energy barrier for nucleation. A processing window was defined, where nucleation was inhibited, and only crystal growth from the particle took place. Here, we found that by adding an acid within a specific range, ZnO deposition can also be localized on a relatively thermal conductive substrate, silicon. Fig. 3a illustrates the deposition area variation after nanowire growth for 1 h by laser irradiation with different amounts of the diluted acid (HNO₃, pH = 2.3). The initial diameter of the ZnO nanoparticle deposition spot

Nanoscale Communication

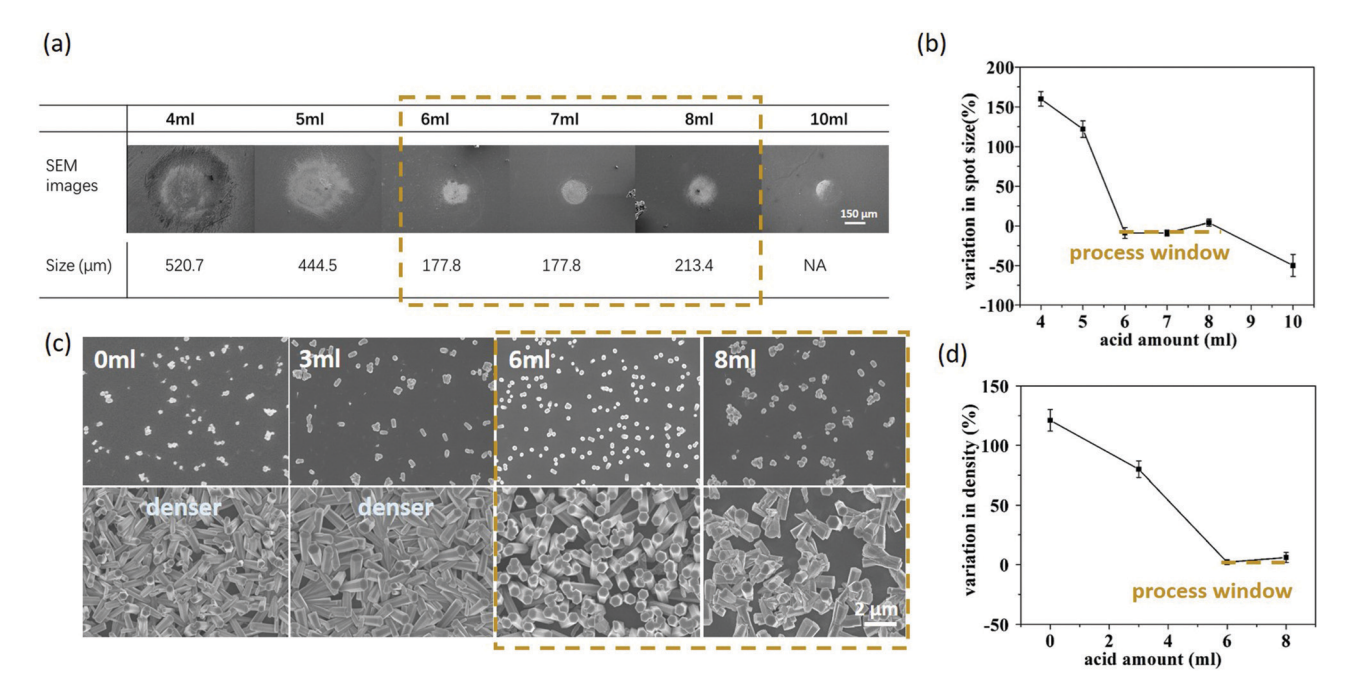


Fig. 3 The process window for controlled integration of ZnO nanowires. (a) SEM images of ZnO spots after 1 h crystal growth process with various amounts of acid (pH = 2.3) from 4 ml to 10 ml. (b) The corresponding line diagram shows the variation of the deposition area before and after nanowire growth in percentage. (c) SEM images of ZnO nanoparticles (top) and the corresponding nanowires (bottom) with various amounts of acid (pH = 2.3) from 0 ml to 8 ml. (d) The corresponding line diagram shows the variation in the percentage of density in the nucleation and nanowire growth processes. The error bars represent the standard error range.

after laser-induced nucleation was around 200 µm. The SEM pictures in Fig. 3(a) show the deposition area after crystal growth. When the amount of acid was less than 6 ml, the delocalization effect on the deposition area was apparent. With 4 ml of acid, the deposition size became 520 μm in diameter. Moreover, with 5 ml of acid, the deposition size was 440 μm. When the amount of acid fell in the window of 6 ml-8 ml (see Fig. 3b), the deposition size almost did not change. When the amount of acid exceeded 10 ml, the existing nanoparticle was partly dissolved, and the deposition area decreased. At this processing window, the nanowire density remained the same compared tothe initial nanoparticle density. The comparison between the original nanoparticle density and nanowire density after 1 h nanowire growth with different amounts of acid is shown in Fig. 3c. When 0-3 ml acid was added to the precursor, the density of nanowires increased compared to the original nanoparticle density, indicating additional nucleation inside the confined area. When an acid was added in the range of 6-8 ml, the nanowire density was approximately the same as the original particle density, which means that nucleation was effectively inhibited in this process window. When acid was added in the range above 10 ml, a large portion of ZnO particles was dissolved by the acid, and the comparison cannot be made. In summary, inside the processing window (6-8 ml of the acid), nanowire growth was decoupled from the nucleation of ZnO in the region outside/inside the laser beam and nanowires with controlled density can be integrated selectively.

Nanowire growth induced by a laser

By taking advantage of the processing window discussed above, nanowires could grow with the desired density. For the first time, the kinetics of laser-induced crystal growth can be studied with density as a controlled variable. According to the ZnO nanowire growth model proposed by Boercker et al.²² when the growth was mass transport limited, the nanowire growth rate was inversely proportional to its number density. Here, we investigated the nanowire growth in two stages: growth after 20 min and growth after 1 h, by exploring the relationship between the nuclei density and nanowire length. The results (8 ml of the acid was added) are shown in Fig. 4a. At the beginning or after 20 min of laser irradiation, the length of crystals grown from nanoparticles with different densities was almost the same. However, after 1 hour of laser irradiation, it was apparent that the nanowires grown from loose nanoparticles were longer and larger. Nanoparticles with average densities of $2.9 \times 10^8 \text{ cm}^{-2}$, $6.4 \times 10^8 \text{ cm}^{-2}$, 10.2×10^8 ${\rm cm}^{-2}$, and 49.6 × 10⁸ ${\rm cm}^{-2}$ were investigated. After 20 min of laser irradiation, the average heights of the nanowires were all around 0.3 µm, independent of the nuclei density. After 1 hour of laser irradiation, the heights of nanowires were 1.3 μm, 0.8 μm, 0.5 μm, and 0.4 μm, respectively. The nanowire height scales as 1/N (N is the area density of the nanowire), as shown in Fig. 4b. According to the model proposed by Boercker et al., the nanowire height-density relationship suggests that the laser-induced growth rate of ZnO was limited by the chemical

Communication Nanoscale

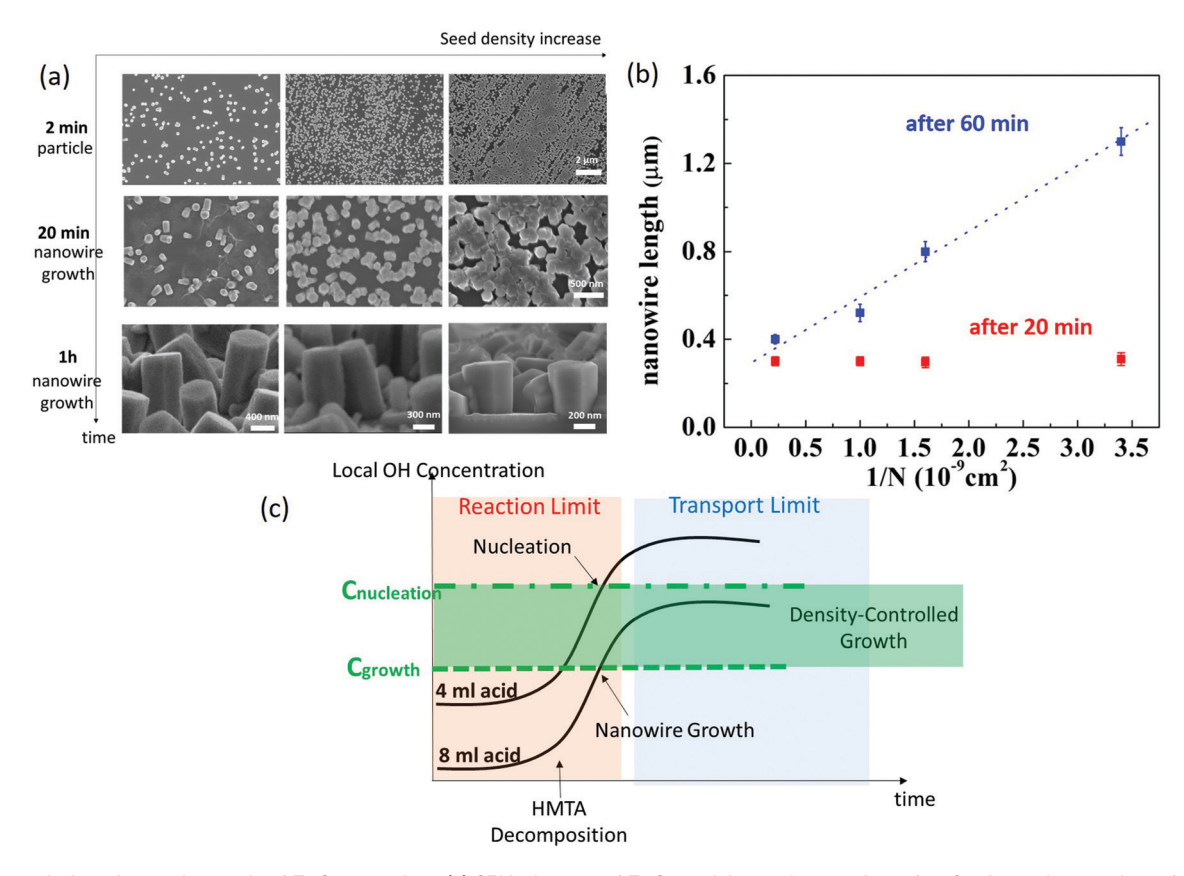


Fig. 4 Laser-induced crystal growth of ZnO nanowires. (a) SEM pictures of ZnO particles and nanowires after 2 min, and nanowires after 20 min, 1 h, respectively, with various densities. (b) The relationship between the nanowire height and nanoparticle density after 20 min and 1 h, respectively. The error bars represent the standard error range. (c) Change of the local OH concentration over time.

reaction at first, and then by mass transport from the bulk solution. Laser heating induced HMTA decomposition and a rise of hydroxide ions locally. The supply of HMTA from the bulk to the reaction zone was sufficient to keep up with the HMTA consumption. As the diffusion layer of HMTA increased, the supply of HMTA became inadequate, and the growth of ZnO nanowires was mass transport limited. We propose that the mass transport limited growth mode is essential for preventing nucleation on new sites during laser-induced crystal growth, as is illustrated in Fig. 4c. The insufficient mass transport kept the OH⁻ ions from accumulating excessively. When 8 ml diluted acid was added to the solution, the initial release of OH helped the local OH concentration to exceed the critical value for crystal growth. Moreover, nanowires began to grow from the existing nanoparticles. As the OH ions in the laser reaction spot accumulated locally, the inadequate precursor supply prevented the local OH concentration to exceed the critical value for nucleation of ZnO. This ensured the maintenance of crystal growth while inhibiting the nucleation. The proposed theory can explain the crystal growth window as discussed earlier. When less diluted acid was added to the solution (4 ml for example), the concentration of OHexceeded the critical value for nucleation before the reaction became transport limited. Subsequently, the size of the deposition/integration area and the density of nanowires increased

as shown in Fig. 3. In this study, the objective is to reveal the mechanism of control integration. Thus, the experimental setting was not optimized (a relatively large amount of acid was used for example) to demonstrate the high growth rate by the laser process shown in previous reports. ^{1,6} The average growth rate demonstrated in this study (0.4–4 μ m h⁻¹) was still higher than that by the conventional non-laser method (about 0.25 μ m h⁻¹ (ref. 22)).

Conclusion

By laser-induced chemical deposition, ZnO nanowires were selectively integrated onto a silicon wafer with a controlled density. The control over nanowire density was realized by decoupling the nanowire growth process from ZnO nucleation on new sites. The discussed mechanisms associated with laser induced chemical deposition are expected to provide important guidance towards potential cost-effective production and integration of various nanomaterial systems.²⁶

Conflicts of interest

There are no conflicts to declare.

Nanoscale Communication

Acknowledgements

The project was partially supported by the NSF (CMMI) Grant 1663214. Note: Some of the ideas in this paper are covered by a pending patent.

References

- 1 Z. Liu and C. Richard Liu, *Manuf. Lett.*, 2013, 1, 42–45.
- 2 Z. Liu and C. R. Liu, J. Micro Nanomanuf., 2014, 2(1), 011001.
- 3 Z. Liu and C. R. Liu, Proc. Inst. Mech. Eng. Part N: J. Nanoeng. Nanosyst., 2013, 228, 66–72.
- 4 Z. Liu, Z. Cao, B. Deng, Y. Wang, J. Shao, P. Kumar, C. R. Liu, B. Wei and G. J. Cheng, *Nanoscale*, 2014, 6, 5853– 5858.
- 5 J. Yeo, S. Hong, M. Wanit, H. W. Kang, D. Lee, C. P. Grigoropoulos, H. J. Sung and S. H. Ko, *Adv. Funct. Mater.*, 2013, 23, 3316–3323.
- 6 J. Bin In, H.-J. Kwon, D. Lee, S. H. Ko and C. P. Grigoropoulos, Small, 2014, 10, 741–749.
- 7 J. Yeo, S. Hong, W. Manorotkul, Y. D. Suh, J. Lee, J. Kwon and S. H. Ko, *J. Phys. Chem. C*, 2014, **118**, 15448–15454.
- 8 J. Yeo, S. Hong, G. Kim, H. Lee, Y. D. Suh, I. Park, C. P. Grigoropoulos and S. H. Ko, *ACS Nano*, 2015, 9, 6059– 6068.
- 9 M. Kwiat, S. Cohen, A. Pevzner and F. Patolsky, *Nano Today*, 2013, 8, 677–694.
- 10 J. A. Liddle and G. M. Gallatin, ACS Nano, 2016, 10(3), 2995–3014.

- 11 H. Lee, W. Manorotkul, J. Lee, J. Kwon, Y. D. Suh, D. Paeng, C. P. Grigoropoulos, S. Han, S. Hong, J. Yeo and S. H. Ko, ACS Nano, 2017, 11, 12311–12317.
- 12 S. Hasegawa, H. Ito, H. Toyoda and Y. Hayasaki, *Opt. Express*, 2016, **24**, 18513.
- 13 A. Gillner, M. Jüngst and P. Gretzki, in *Advanced Solid State Lasers*, OSA, Washington, D.C., 2015, p. AF3A.5.
- 14 M. Silvennoinen, J. Kaakkunen, K. Paivasaari and P. Vahimaa, *Opt. Express*, 2014, 22, 2603.
- 15 X. D. Wang, J. Zhou, C. S. Lao, J. H. Song, N. S. Xu and Z. L. Wang, *Adv. Mater.*, 2007, **19**, 1627–1631.
- 16 W. Z. Wu, X. N. Wen and Z. L. Wang, Science, 2013, 340, 952–957.
- 17 C. H. Liu, J. A. Zapien, Y. Yao, X. M. Meng, C. S. Lee, S. S. Fan, Y. Lifshitz and S. T. Lee, *Adv. Mater.*, 2003, 15, 838–841.
- 18 R. H. Zhang, E. B. Slamovich and C. A. Handwerker, *Nanotechnology*, 2013, 24, 195603.
- 19 S. E. Skrabalak and Y. Xia, ACS Nano, 2009, 3, 10-15.
- 20 X. Liu, Y.-Z. Long, L. Liao, X. Duan and Z. Fan, ACS Nano, 2012, 6, 1888–1900.
- 21 K. Govender, D. S. Boyle, P. B. Kenway and P. O'Brien, J. Mater. Chem., 2004, 14, 2575–2591.
- 22 J. E. Boercker, J. B. Schmidt and E. S. Aydil, *Cryst. Growth Des.*, 2009, **9**, 2783–2789.
- 23 Y. G. Wei, W. Z. Wu, R. Guo, D. J. Yuan, S. Das and Z. L. Wang, *Nano Lett.*, 2010, 10, 3411.
- 24 J. J. Cheng, S. M. Nicaise, K. K. Berggren and S. Gradečak, Nano Lett., 2016, 16, 753–759.
- 25 B. Weintraub, Z. Zhou, Y. Li and Y. Deng, *Nanoscale*, 2010, 2, 1573–1587.
- 26 Z. Y. Lin, Y. Zhao, C. J. Zhou, R. Zhong, X. Wang, Y. H. Tsang and Y. Chai, Sci. Rep., 2015, 5, 18596.